energies

MDPI

Article

Modeling of Turbulent Heat-Transfer Augmentation in Gas-Droplet Non-Boiling Flow in Diverging and Converging Axisymmetric Ducts with Sudden Expansion

Maksim A. Pakhomov * and Viktor I. Terekhov

Laboratory of Thermal and Gas Dynamics, Kutateladze Institute of Thermophysics, Siberian Branch of Russian Academy of Sciences, Acad. Lavrent'ev Avenue 1, 630090 Novosibirsk, Russia
* Correspondence: pakhomov@ngs.ru

Abstract: The effect of positive (adverse) and negative (favorable) longitudinal pressure gradients on the structure and heat transfer of gas-droplet (air and water) flow in axisymmetric duct with sudden expansion are examined. The superimposed pressure gradient has a large influence on the flow structure and heat transfer in a two-phase mist flow in both a confuser and a diffuser. A narrowing of the confuser angle leads to significant suppression of flow turbulence (more than four times that of the gas-drop flow after sudden pipe expansion without a pressure gradient at $\varphi = 0^\circ$). Recirculation zone length decreases significantly compared to the gas-droplet flow without a longitudinal pressure gradient (by up to 30%), and the locus of the heat-transfer maximum shifts slightly downstream, and roughly aligns with the reattachment point of the two-phase flow. Growth of the diffuser opening angle leads to additional production of kinetic energy of gas flow turbulence (almost twice as much as gas-droplet flow after a sudden pipe expansion at $\varphi = 0^\circ$). The length of the flow recirculating region in the diffuser increases significantly compared to the separated gas-droplet flow without a pressure gradient ($\varphi = 0^\circ$), and the location of maximum heat transfer shifts downstream in the diffuser.

Keywords: heat transfer; droplets evaporation; turbulence; droplet-laden flow; confuser; diffuser; pipe; sudden expansion; RANS

Citation: Pakhomov, M.A.; Terekhov, V.I. Modeling of Turbulent Heat-Transfer Augmentation in Gas-Droplet Non-Boiling Flow in Diverging and Converging Axisymmetric Ducts with Sudden Expansion. *Energies* **2022**, *15*, 5861. https://doi.org/10.3390/en15165861

Academic Editor: Gianpiero Colangelo

Received: 11 July 2022
Accepted: 9 August 2022
Published: 12 August 2022

1. Introduction

Two-phase flows in pipes or channels with a backward-facing step (BFS) are often used in energy and chemical equipment. They have a rather simple flow geometry and are one of the classical types of shear flows, but their flow structure is quite complex. A flow detaches from the sharp edge at the flow SE station, thus forming a region of shear mixing layer. A large recirculation flow region (a few step heights) develops (see comprehensive reviews [1,2]).

The complexity of modeling flow and heat transfer is exacerbated after BFS in the presence of a longitudinal pressure gradient (LPG) in an expanding (diffuser) or narrowing (confuser) subsonic turbulent two-phase flow (see Figure 1). An overview of the state of research on flows in a diffuser or confuser without sudden expansion of a pipe [3] or a channel [4,5] has been presented. The study of the effect of LPG behind a pipe or channel with SE on mean and fluctuational flow and heat transfer is an important for mechanical engineering. There are several studies on the development of separated flows with the influence of longitudinal pressure gradient for a single-phase flow, yet only a few of these experimental works concerned the flow in diffusers and confusers with a BFS [6–9].

An effect of flow separation in the field of LPG was experimentally evaluated in said studies. The position of an "upper" duct wall was changed, which caused narrowing or expansion of a cross-section, whereas the "lower" wall with the SE remained unchanged. The most detailed structures of the turbulent flow were assessed in [6] using the LDA method along the length of the diffuser channel. The authors measured the profiles of

averaged longitudinal and transverse velocities and their fluctuations, Reynolds stresses, length of the recirculation region, triple correlations, and turbulent viscosity. The authors then compared their experimental and numerical data.

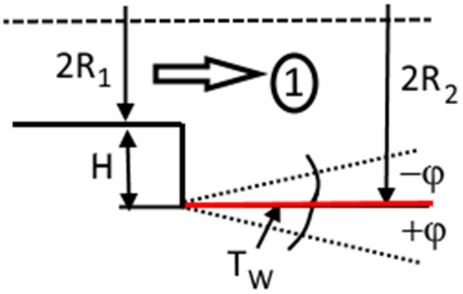

Figure 1. Schematic view of the flow in diffuser (APG, $+\varphi$), confuser (FPG, $-\varphi$), and in the separated flow in pipe sudden expansion (ZPG, $\varphi = 0$). 1 is the droplet-laden flow.

The experimental results on the effect of favorable pressure gradient (FPG) and adverse pressure gradient (APG) in a channel behind a BFS on heat transfer and wall pressure distributions at Reynolds numbers $Re_H = U_{m1}H/\nu = (0.4–1.2) \times 10^4$ were presented in [10]. The diffuser opening angle varied in the range of $\varphi = 0–4°$, and confuser narrowing angle was varied within $\varphi = 0–-7.5°$. The magnitude of the Nusselt number increases as the LPG increases for a narrowing channel, and it decreases for the diffuser. The locus of the heat-transfer maximum moves downstream with diffuser expansion, and shifts upstream towards the step as the confuser narrows. In [11], a quantitative study assessed the effect of an APG on mean flow, turbulence, and heat transfer in an axisymmetric diffuser in a pipe with SE. The literature also presents experimental [12] and numerical [13–18] studies of fluid flow and heat transfer in single-phase turbulent flows without SE of a pipe or channel in the presence of APG and FPG for a single-phase flow.

Solid particles addition to a turbulent flow in a BFS have large effect on reduction of turbulent kinetic energy (TKE) in backward-facing step flow [19]. Droplets evaporation in turbulent flow behind a BFS [20] or after a pipe with SE [21] causes significant intensification of heat transfer (by several times in comparison with a single-phase flow). Authors of this work have published numerical investigations of heat-transfer augmentation in gas-droplet flows behind a pipe with SE [21]. There are few papers concerning numerical simulation of gas-liquid flow [22,23] and droplet-laden [24] flows in a converge or divergent channel without sudden expansion; we know of only one work on the numerical study of heat transfer in two-phase flows after pipe sudden expansion with LPG [25], where the effect of evaporation of water droplets on heat transfer in an axisymmetric diffuser was studied. Heat transfer in turbulent droplet-laden flow with SE with APG and FPG has not been previously performed. The influence of LPG on flow and heat transfer in the confuser and diffuser after pipe SE is evaluated in the present study.

2. Mathematical Methods and Numerical Solution

The motion and heat transfer of a two-phase turbulent gas-droplet flow in a pipe with SE is numerically considered. A sketch of the flow is given in Figure 1. To simulate the dispersed phase dynamics, the Eulerian approach [26–28] is used. The Eulerian approach is widely used for the simulations of two-phase confined flows [21,22,29,30]. The system of axisymmetric stationary Reynolds-averaged Navier–Stokes (RANS) equations accounts for the effect of vaporizing drops on mean and fluctuational transport processes [21,25]. The set of governing equations both for gas and dispersed phases have been provided in detail [21,25]. The volume fraction of the droplets is low ($\Phi_1 = M_{L1}\rho/\rho_L < 1.2 \times 10^{-4}$ for the highest mass fraction studied $M_{L1} = 10\%$). Drops are rather small ($d_1 < 100$ μm), so effects of their collisions can be neglected. Gas phase turbulence is predicted using the elliptical Reynolds stress model [31] by taking the dispersed phase influence on TKE [32].

Break-up and coalescence of droplets in flow is not taken into account due to their rarity ($\Phi_1 < 1.2 \times 10^{-4}$) [33]. The Weber number $We = \rho(\mathbf{U}_S - \mathbf{U}_L)^2 d/\sigma << 1$ and the bag break-up are ignored [33,34]. Here, $\mathbf{U}_S = \mathbf{U} + \langle u'_S \rangle$ is the gas velocity seen by the droplet, and $\langle u'_S \rangle$ is the drift velocity between fluid flow and drops [35]. This assumption is applicable when the pipe cross-section expands for a diffuser. The use of this approach seems less obvious for a confuser, even when taking into account the preliminary pipe with SE. Effect of break-up and coalescence in the flow can be neglected due to a low droplet volume fraction at the inlet according to preliminary author's estimations.

The technique for numerical implementation of the Eulerian approach for two phases is described in detail in [21,25]. The numerical solution was obtained using the finite volume method on staggered grids. The QUICK scheme of third-order ode accuracy was utilized for solution of convective terms. Central differences of second-order accuracy were evaluated for diffusion fluxes. Pressure–velocity fields were corrected according to SIMPLEC procedure.

All simulations were carried out on a "basic" mesh containing 550 × 200 control volumes (CV) for the diffuser with the largest opening angle, and for the confuser with the largest convergence angle of 550 × 100. The information about meshes for the confuser and diffuser is summarized in Table 1. The difference in calculations of the Nusselt number for the two-phase gas-droplet flow did not exceed 0.1%. A further increase in their number does not significantly affect the results of numerical calculations. The grid verification for the case of droplet-laden flow in pipe with SE was presented in [21]. The grid independence tests for two-phase flows in APG and FPG are given in Figure 2 for the smallest constriction angle in the confuser and for the largest opening angle in diffuser. The Nusselt number at a constant wall temperature is determined by dependence:

$$\mathrm{Nu} = -(\partial T/\partial y)_W H/(T_W - T_m),$$

where T_m is mass-averaged temperature of gas in the considered cross-section.

Table 1. Meshes for two-phase flow in the confuser (FPG) and diffuser (APG).

Flow Type	"Basic"	"Coarse"	"Fine"
Confuser	550 × 100	300 × 50	850 × 150
Diffuser	550 × 200	300 × 100	850 × 300

The convergence criteria for all residual levels in this study were up to 10^{-5}. The differences in Nusselt number and gas-phase kinetic energy of turbulence for gas-droplet APG and FPG flows were up to 10^{-6}.

The model was validated against experimental results on the flow and heat transfer for the single-phase axisymmetric diffuser downstream of a pipe with SE. The difference between our predictions and measured results of previous experiments did not exceed 15%. These results were given in our previous paper [25], but this comparison is not presented here. We did not find measured or numerical results concerning the study of an APG or FPG of gas-droplet flow in a pipe or duct with sudden expansion. We performed the comparisons with experimental two-phase droplet-laden mist and solid particle-laden turbulent flow behind the BFS and a pipe with SE. These results were published in a previous paper [21] but are not included here. We believe that the validation analysis of two-phase solid particle-laden and droplet-laden flows behind backward-facing step or pipe sudden expansion without LPG have been fully completed.

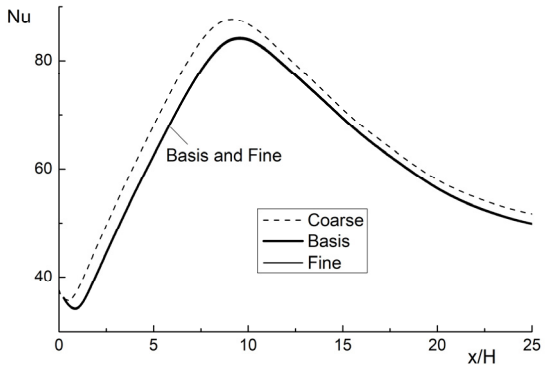

(**a**)

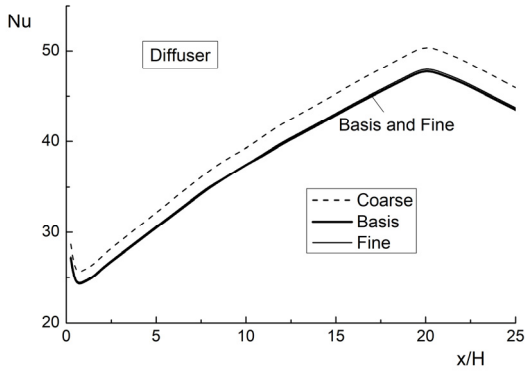

(**b**)

Figure 2. Grid independence tests for confuser at $\varphi = -1^\circ$ (**a**) and diffuser at $\varphi = 5^\circ$ (**b**).

3. Results and Discussion

The primary concern of this study was shown the effect of diffuser opening and confuser narrowing angles on the characteristics and heat transfer in the two-phase mist with vaporized water droplets after the pipe with SE. Drop diameter and mass fraction decreased due to evaporation both in the axial and radial directions after the flow detachment section.

The diffuser expanding angle was φ = 0–5° and the confuser convergence angle φ = 0–−3°. The pipe diameter before SE was $2R_1$ = 20 mm, after SE it was $2R_2$ = 60 mm, and the step height was H = 20 mm. The computational domain after pipe expansion was $25H$ = 0.5 m. Mass-average air velocity before separation was U_{m1} = 15 m/s, and the Reynolds number was $\mathrm{Re}_H = HU_{m1}/\nu \approx 2 \times 10^4$. The wall temperature was T_W = const = 373 K, and the temperatures of air and droplets at the inlet were $T_1 = T_{L1}$ = 293 K. Water droplets were added to a single-phase air turbulent flow at the inlet, and their initial velocity was set constant over pipe cross-section: $U_{L1} = 0.8U_{m1}$. Inlet droplet size was constant d_1= 1–100 μm, and mass fraction M_{L1} = 0.01–0.1. The Stokes number in mean motion was Stk = τ/τ_f = 0.03–3, where $\tau_f = 5H/U_{\mathrm{m1}}$ is the turbulent time macroscale [19,20]. Here, $\tau = \rho_L d^2/(18\rho\nu W)$ is the particle relaxation time, $W = 1 + \mathrm{Re}_L^{2/3}/6$ and $\mathrm{Re}_L = |\mathbf{U}_S - \mathbf{U}_L|d/\nu$ is the dispersed-phase Reynolds number. The Stokes number $\mathrm{Stk}_K = \tau/_{fK}$ = 0.2–20, where τ_K is the Kolmogorov timescale. While the value of interfacial velocity in our previous works [21,25] was based only on the average velocity of the carrier phase, it is based on the actual value in the present study.

3.1. The Wall Friction and Pressure Coefficients

The distributions of wall friction coefficient $C_f/2 = \tau_W/\left(\rho U_{m1}^2\right)$ and pressure coefficient $C_P = 2(P_W - P_1)/\left(\rho U_{m1}^2\right)$ along the length of diffuser and confuser in gas-droplet

flow with variation of expansion and contraction angles are shown in Figure 3. Here, τ_W is the wall friction; P_W, P_1 are the mean static pressures on the wall in considered and inlet cross-sections. The data for the flow after a pipe with SE, without an effect of LPG ($\varphi = 0°$), are also shown in this figure for comparison.

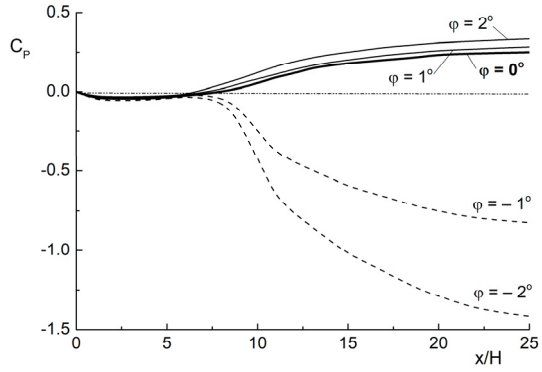

(**a**)

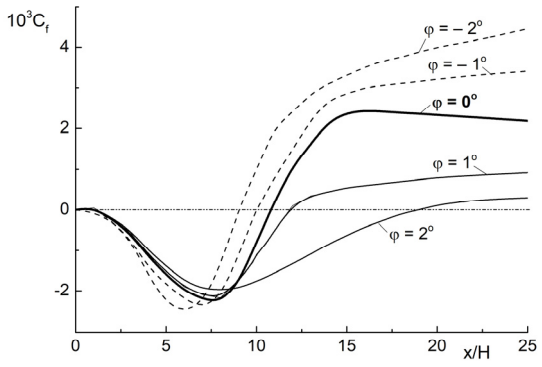

(**b**)

Figure 3. The evolution of pressure C_P (**a**) and wall friction C_f (**b**) coefficients along the axial coordinates in ZPG ($\varphi = 0°$), diffuser ($\varphi > 0°$, APG), and confuser ($\varphi < 0°$, FPG). $M_{L1} = 0.05$, $d_1 = 30$ μm.

The distributions of non-dimensional pressure coefficients along axial coordinates with the development of a separated flow in the diffuser and confuser are shown in Figure 3a. In the diffuser, directly behind the flow separation point, a negative pressure region is formed, with a length of $x/H \approx 7$. The pressure coefficient also increases with an increase in the diffuser opening angle, which can be attributed mainly to flow deceleration. The zone with pressure attenuation is formed in the confuser directly behind the flow detachment cross-section, and its length axial direction is x/H = 5–7. With growth of the confuser convergence angle, the presence of a significant region of pressure attenuation is observed, and the absolute value of pressure attenuation increases noticeably as the convergence angle increases (more than 5.5 times at $\varphi = -2°$). Obviously, the main reason for a significant pressure decrease in confuser is flow acceleration. The wall friction coefficient C_f decreases significantly (several times over) with growth of APG, and a sharp increase in the flow recirculation zone is observed (see Figure 3b). With the increase in the magnitude of FPG, the wall friction coefficient increases noticeably (almost doubling) after the zone of flow relaxation.

3.2. The Flow Structure in Confuser (FPG) and Diffuser (APG)

Profiles of the mean axial velocity, temperature, and turbulent kinetic energy of the gas phase in a cross-section at x/H = 15 are shown in Figure 4. The predictions are carried out for different values for the diffuser (APG, $\varphi > 0°$), the confuser (FPG, $\varphi < 0°$), and in the

separated flow behind sudden expansion of the pipe ($\varphi = 0°$). A large effect of two-phase flow detachment with a zero pressure gradient (ZPG) and with FPG and APG on the mean axial velocity distributions is revealed in two-phase flow. Obviously, the increase in the diffuser opening angle leads to a reduction of gas velocity in the core zone (see Figure 4a). It should be noted that in a cylindrical duct, as well as at small diffuser opening angles ($\varphi \leq 2°$), the separated flow is reattached in cross-section ($x/H = 15$) and the flow is relaxed. Air velocity and the velocity gradient in the radial direction in the core region increase in the confuser.

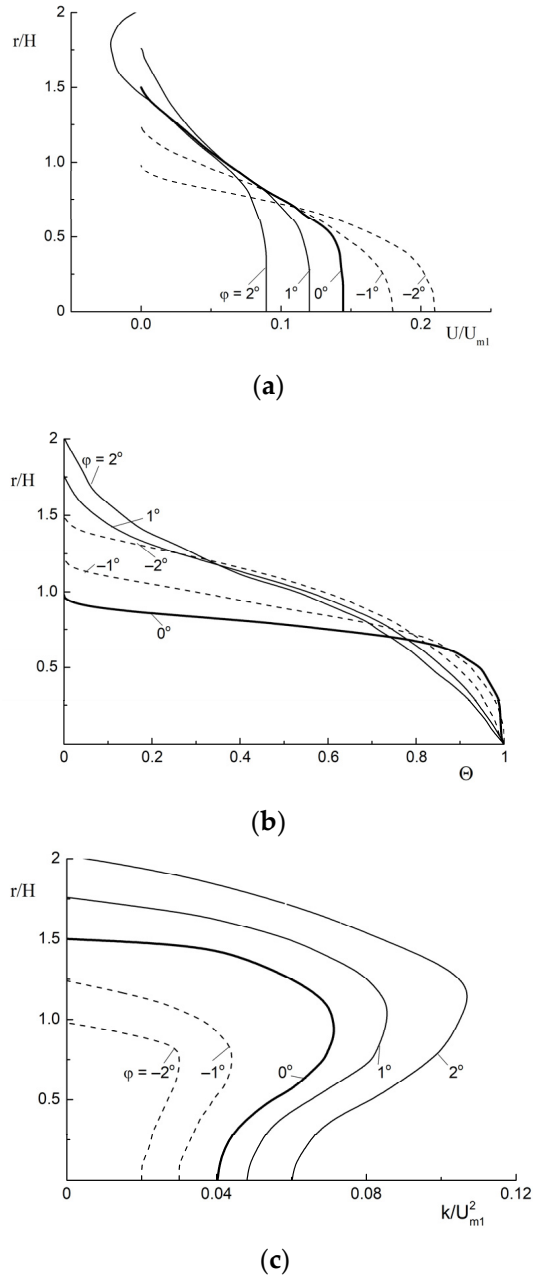

Figure 4. Mean streamwise velocity component (**a**), temperature (**b**), TKE (**c**) of the gas phase in ZPG ($\varphi = 0°$), confuser (FPG, $\varphi < 0°$), and diffuser (APG, $\varphi > 0°$). The results for the confuser are the dashed lines, for the diffuser are the solid curves, and the separated flow with $\varphi = 0°$ are the bolded lines. $M_{L1} = 0.05$, $d_1 = 30$ μm.

Gas temperature distributions $\Theta = (T - T_W)/(T_0 - T_W)$ over the pipe radius depend, to a lesser extent, on the longitudinal pressure gradient rather than on distributions of the

axial gas velocity (see Figure 4b). Here, T_0 and T_W are gas phase temperatures on a pipe axis and on a wall. The slightly changing diverging angle of the diffuser ($\varphi \leq 2^\circ$) and the converging angle of the confuser ($\varphi \geq -2^0$) have little effect on the gas phase temperature in droplet-laden flow. The temperature increases for the diffuser and decreases for the confuser. This leads to heat-transfer enhancement in the confuser and heat-transfer suppression in the diffuser. These conclusions qualitatively concur with the results of simulations [11] for a single-phase flow in a diffuser behind a pipe with SE. Gas temperature becomes lesser for gas-droplet flow compared to the case at $\varphi = 0^\circ$.

Turbulent kinetic energy (TKE) of the gaseous phase is significantly enhanced (by up to two times over) by an increase in the diffuser opening angle (see Figure 4c). The TKE of the gas phase is calculated for an axisymmetric flow using a known formula: $2k = \langle u'^2 \rangle + \langle v'^2 \rangle + \langle w'^2 \rangle \approx \langle u'^2 \rangle + 2\langle v'^2 \rangle$. This is not an effect of the dispersed phase; it is known that the presence of a finely dispersed phase suppresses the carrier-phase turbulence in the separated flow, both behind the BFS [19,20] and with sudden expansion of the pipe [21,22]. Particles or droplets are involved in the mean gas movement and a part of the turbulent energy of a carrier flow is spent on this process [19,32]. The maximum kinetic energy of turbulence is observed in the mixing layer, and the same phenomena were found for the gas-droplet flow in the pipe with sudden expansion at ZPG ($\varphi = 0^\circ$) [21]. This effect was shown previously, in our recent study of an axisymmetric diffuser with a sudden pipe expansion [25]. An increase in the LPG in an axisymmetric diffuser with pipe SE causes additional flow turbulization. The maximum value of the turbulent kinetic energy of the carrier phase for a confuser decreases almost twice as much compared to the turbulence level of a separated two-phase flow at ZPG. Such a significant TKE suppression of the carrier phase cannot be explained only by the effect of the dispersed phase.

The transverse distributions of mean axial water droplet velocity U_L/U_{L1} (a), drops in temperature $\Theta_L = (T_L - T_{L,\max})/(T_{L,0} - T_{L,\max})$ (b), and the mass fraction M_L/M_{L1} (c) of dispersed phase in the confuser and diffuser in a pipe with SE are presented in Figure 5. Here T_L, T_L, and $T_{L,\max}$ are the droplet temperature, the droplet temperature on pipe axis, and maximum droplet temperature in corresponding cross-section, respectively.

With growth of the confuser convergence angle, a significant increase in the longitudinal averaged velocity of droplets occurs (by more than double at $\varphi = -2^\circ$ as compared to the separated flow at ZPG) (see Figure 5a). The droplet temperature profile has a qualitatively similar form for all three types of ducts (ZPG, APG, and FPG) studied previously (see Figure 5b). On the whole, droplet temperature distributions are similar to those for the gas phase. The maximum value of droplet mass fraction is obtained in the axial region of the pipe, and the minimum value is obtained in its near-wall region (see Figure 5c). The simulations for droplets' mass fractions $M_{L1} > 10\%$ were not successful due to the possible effect of droplets deposition in reality. Most likely, the distribution of the mass fraction of droplets is qualitatively similar to those for $M_{L1} = 10\%$, but there are quantitative differences. It is also necessary to take into account the effect of droplet deposition on the wall from a two-phase flow, and the possible formation of liquid spots and films on the wall surface. The influence of droplet deposition on transport processes and heat transfer are not taken into account for our numerical results obtained for $M_{L1} = 5\%$. Obviously, for high values of the droplets' mass fraction at the inlet, it is necessary to account for the influence of the deposition process and the entrainment of liquid droplets into the droplet-laden flow from the liquid film or spots.

3.3. The Effect of LPG on the Mean Parametrs of the Two-Phase Mist Flow

A significant increase in the length of recirculating area x_R is observed in two-phase flow in diffuser (see Figure 6). The locus of the heat-transfer peak $x_{\max}$ moves in the downstream direction. A slight increase in the flow recirculation region is shown for small expanding angles ($\varphi \leq 1^\circ$), and the position of the heat-transfer maximum is close to the locus of the reattachment point of two-phase flow. The coordinate of $x_{\max}$ moves downstream by almost double ($\varphi = 5^\circ$) in comparison with the case of $\varphi = 0^\circ$. The presence

of FPG leads to a reduction in flow recirculation area and the coordinates of $x_{\max}$ move upstream by about 30–35% compared to the case of $\varphi = 0^\circ$. The significant displacement of flow reattachment points in the diffuser and confuser is caused by deformation of the gas phase velocity profile due to the effect of LPG.

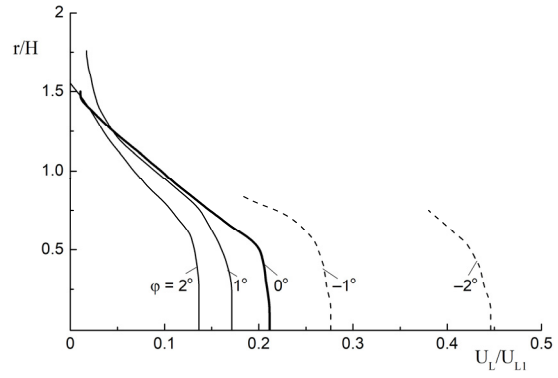

(**a**)

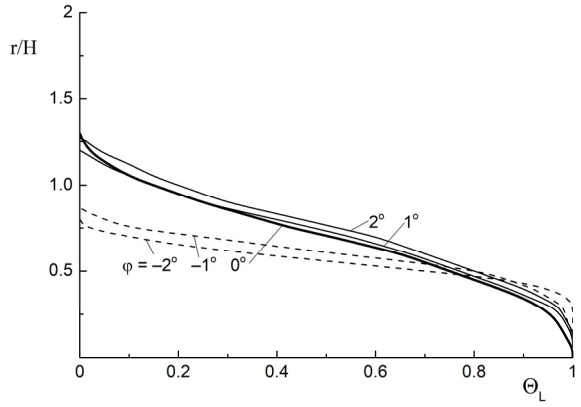

(**b**)

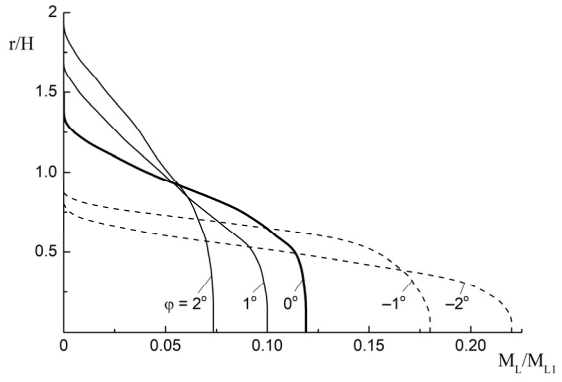

(**c**)

Figure 5. Mean axial velocity componet (**a**), temperature (**b**), and mass fraction (**c**) of the dispersed phase. The results for confuser (FPG, $\varphi < 0^\circ$) are the dashed lines, for the diffuser (APG, $\varphi > 0^0$) are the solid curves, and the separated flow with $\varphi = 0^\circ$ are the bold lines. $M_{L1} = 0.05$, $d_1 = 30$ μm.

The TKE of the carrier phase increases almost two times over in the diffuser at $\varphi = 5^\circ$ as compared with the case without longitudinal pressure gradient $\varphi = 0^\circ$. Changing the confuser convergence angle causes suppression of the level of turbulence more than three times over. The heat transfer decreases significantly with expanding of diffuser opening angle (almost by a factor of 1.5 as compared to the separated flow in the pipe at $\varphi = 0^\circ$).

For the confuser, an increase in the relative value of the maximum heat transfer is observed at $\varphi = -3^\circ$ (by approximately 20%). The heat transfer for the confuser (FPG) case has the greatest value, and the diffuser (APG) has the smallest.

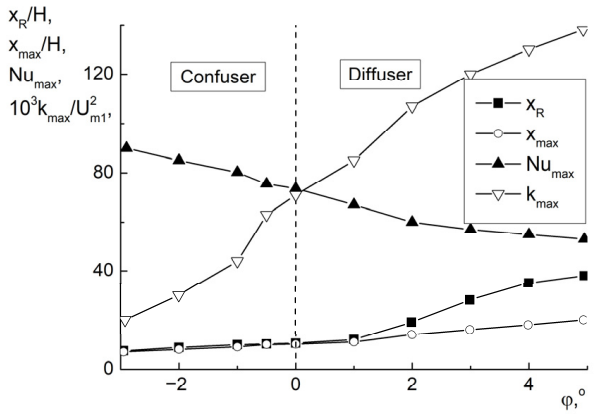

Figure 6. Effect of LPG on recirculating length x_R, location of heat transfer maximum $x_{\max}$, value of maximal Nusselt number $\mathrm{Nu}_{\max}$, and maximum of TKE $k_{\max}$ in gas-droplet flow in pipe SE. $M_{L1} = 0.05$, $d_1 = 30$ μm.

The effect convergence (confuser) and divergence (diffuser) on Nusselt number distributions along the axial coordinate for the separated flow (ZPG), confuser (FPG), and diffuser (APG) are shown in Figure 7. Initially, for two-phase mist flows with APG and FPG, the attenuation of heat transfer rate is observed. This is typical both for both types of flows and for the case of gas-droplet flow in pie with SE at $\varphi = 0^\circ$. Then there is a sharp increase in heat transfer with the achievement of a maximum heat transfer. In the zone of flow relaxation, the observed decrease in Nusselt number is similar to a single-phase flow.

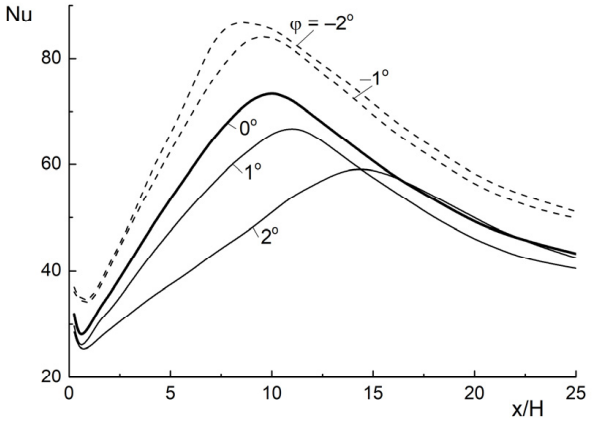

Figure 7. Nusslet numbers distributions along streamwise coordinate in ZPG ($\varphi = 0^\circ$), FPG ($\varphi < 0^\circ$), and APG ($\varphi > 0^\circ$). $M_{L1} = 0.05$, $d_1 = 30$ μm.

The influence of water droplets' mass concentration on the maximal magnitude of heat transfer $\mathrm{Nu}_{\max}$ for a diffuser and confuser after pipe SE is presented in Figure 8. For all types of flow behind the pipe with SE at $\varphi = 0^\circ$, in the diffuser ($\varphi = 2^\circ$), and in the confuser ($\varphi = -2^\circ$), an increase in the maximum heat-transfer value (up to 75% in a single-phase airflow) was obtained with increasing mass fraction of droplets to $M_{L1} = 10\%$. The heat transfer in confuser enhances compare to the diffuser and for two-phase separated flow with ZPG at $\varphi = 0^\circ$.

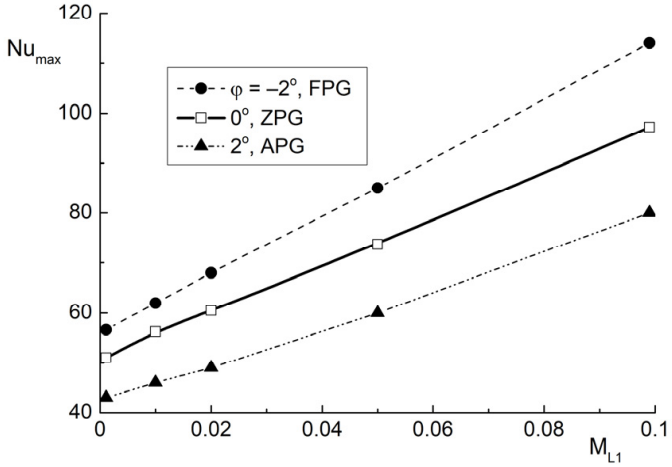

Figure 8. The magnitude of maximal heat transfer in the diffuser ($\varphi = 2^\circ$), confuser ($\varphi = -2^\circ$) and separated flow ($\varphi = 0^\circ$) vs water droplets mass concentration. $d_1 = 30$ μm.

4. Conclusions

The numerical results of the effects of favorable and adverse longitudinal pressure gradients on the flow and heat transfer augmentation, in a droplet-laden flow in a pipe with SE, are presented. Elliptical second-moment closure was used to predict the gas phase turbulence with taking into account the effect of droplets presence. While this study does not have a direct application, it shows potential ways to control the turbulence level and to enhance heat transfer performance in APG and FPG flow behind a backward-facing step. Thus, these data may be of interest for various practical applications. The scope of the model's use is limited the inlet droplet diameter $d_1 = 100$ μm and their initial mass fraction $M_{L1} \leq 10\%$. This can be explained by noting that the model does not take into account the formation and evolution of a liquid film on the pipe wall, as drops break up and coalesce.

The presence of flow expansion (diffuser) and constriction (confuser) of pipe with SE shows significant effect on the mean and fluctuational flow characteristics, and heat transfer in an axisymmetric. The increase of the confuser constriction angle causes considerable reduction of the pressure coefficient. The length of the flow recirculating area noticeably shortens compared to the gas-droplet flow behind the pipe with SE at angle $\varphi = 0^\circ$, and the point of maximum of heat transfer slightly shifts downstream. The heat transfer augmentation and the suppression of turbulence in a two-phase flow in a confuser are mainly due to the FPG. The large growth of flow recirculating area (up to 3.5 times at $\varphi = 5^\circ$) compared to the gas-droplet flow downstream of pipe SE at $\varphi = 0^\circ$ is obtained. The expansion of the diffuser leads to reduction of the wall friction coefficient. Two-phase flow does not reattach to the wall at angle $\varphi = 5^\circ$. Points of flow reattachment and maximum heat transfer are significantly shifted downstream by an increase in the opening angle of the diffuser. The significant heat-transfer suppression (by up to 1.5 times) and turbulence production (by up to two times) are observed for the two-phase mist flow in a diffuser.

Author Contributions: Conceptualization, M.A.P. and V.I.T.; methodology, M.A.P. and V.I.T.; Investigation, M.A.P.; data curation, M.A.P. and V.I.T.; formal analysis, M.A.P. and V.I.T.; writing—original draft preparation, M.A.P. and V.I.T.; writing—review and editing, M.A.P. and V.I.T.; resources, M.A.P. and V.I.T.; project administration, V.I.T. All authors have read and agreed to the published version of the manuscript.

Funding: This work was financially supported by the grant of the Russian Science Foundation (project code 21-19-00162).

Institutional Review Board Statement: Not applicable.

Informed Consent Statement: Not applicable.

Conflicts of Interest: The authors declare no conflict of interest.

Nomenclature

d	droplet diameter
H	step height
M_L	mass fraction
$\mathrm{Nu} = -(\partial T/\partial y)_W H/(T_W - T_m)$	Nusselt number
$\mathrm{Re}_H = U_{m1} H/\nu$	Reynolds number
$\mathrm{Stk} = \tau/\tau_f$	mean Stokes number
T	temperature
$\mathbf{U}$	average velocity vector
U_i, U_j	mean gas velocities components
$\mathbf{U}_S = \mathbf{U} + \langle u'_S \rangle$	gas velocity vector seen by the droplet
$\langle u'_S \rangle$	drift velocity between fluid flow and drops
$\mathrm{We} = \rho(\mathbf{U}_S - \mathbf{U}_L)^2/\sigma$	Weber number
x	streamwise coordinate
$x_{\max}$	location of heat-transfer maximum
x_R	reattachment length
Subscripts	
0	single-phase fluid (air) flow
1	initial condition
L	liquid
m	mean
max	maximal value
W	wall
Greek	
Φ	volume fraction
λ	thermal conductivity
ρ	density
ν	kinematic viscosity
τ	particle relaxation time
τ_W	wall shear stress
φ	diffuser opening angle ($\varphi > 0$) or confuser ($\varphi < 0$) narrowing angle
Acronym	
APG	adverse pressure gradient
BFS	backward-facing step
FPG	favorable pressure gradient
LPG	longitudinal pressure gradient
CV	control volume
SE	sudden expansion
ZPG	zero pressure gradient

References

1. Eaton, J.K.; Johnston, J.P. A review of research on subsonic turbulent flow reattachment. *AIAA J.* **1981**, *19*, 1093–1100. [CrossRef]
2. Chen, L.; Asai, K.; Nonomura, T.; Xi, G.N.; Liu, T.S. A review of backward-facing step (BFS) flow mechanisms, heat transfer and control. *Thermal Sci. Eng. Progr.* **2018**, *6*, 194–216. [CrossRef]
3. Klein, A. Review: Effects of inlet conditions on conical-diffuser performance. *ASME J. Fluids Eng.* **1981**, *103*, 250–257. [CrossRef]
4. Azad, R.S. Turbulent flow in a conical diffuser: A review. *Exp. Therm. Fluid Sci.* **1996**, *13*, 318–337. [CrossRef]
5. Apsley, D.D.; Leschziner, M.A. Advanced turbulence modelling of separated flow in a diffuser. *Flow Turbul. Combust.* **1999**, *63*, 81–112. [CrossRef]
6. Driver, D.M.; Seegmiller, H.L. Features of a reattaching turbulent shear layer in divergent channel flow. *AIAA J.* **1985**, *23*, 163–171. [CrossRef]
7. Ra, S.H.; Chang, P.K. Effects of pressure gradient on reattaching flow downstream of a rearward-facing step. *J. Aircr.* **1990**, *27*, 93–95. [CrossRef]
8. Iftekhar, H.; Agelin-Chaab, M. Structure of turbulent flows over forward facing steps with adverse pressure gradient. *ASME J. Fluids Eng.* **2016**, *138*, 111202. [CrossRef]
9. Wang, L.B.; Tao, W.Q.; Wang, Q.W.; Wong, T.T. Experimental study of developing turbulent flow and heat transfer in ribbed convergent/divergent square ducts. *Int. J. Heat Fluid Flow* **2001**, *22*, 603–613. [CrossRef]

10. Terekhov, V.; Dyachenko, A.; Smulsky, Y. The effect of longitudinal pressure gradient on heat transfer in a separated flow behind a sudden expansion of the channel. *Heat Transf. Eng.* **2020**, *41*, 1404–1416.
11. Terekhov, V.I.; Bogatko, T.V. Aerodynamics and heat transfer in a separated flow in an axisymmetric diffuser with sudden expansion. *J. Appl. Mech. Techn. Phys.* **2015**, *56*, 471–478. [CrossRef]
12. Güemes, A.; Sanmiguel Vila, C.; Örlü, R.; Vinuesa, R.; Schlatter, P.; Ianiro, A.; Discetti, S. Flow organization in the wake of a rib in a turbulent boundary layer with pressure gradient. *Exp. Therm. Fluid Sci.* **2019**, *108*, 115–124. [CrossRef]
13. Leont'ev, A.I.; Lushchik, V.G.; Reshmin, A.I. Heat transfer in conical expanding channels. *High Temp.* **2016**, *54*, 270–276. [CrossRef]
14. Lushchik, V.G.; Reshmin, A.I. Heat transfer enhancement in a plane separation-free diffuser. *High Temp.* **2018**, *56*, 569–575. [CrossRef]
15. Lushchik, V.G.; Makarova, M.S.; Reshmin, A.I. Laminarization of flow with heat transfer in a plane channel with a confuser. *Fluid Dyn.* **2019**, *54*, 67–76. [CrossRef]
16. Sakhnov, A.Y. Local laminarization within the mild pressure gradient flow over the heated wall. *Int. J. Heat Mass Transf.* **2021**, *165*, 120698. [CrossRef]
17. Sakhnov, A.Y.; Naumkin, V.S. Velocity overshoot within the accelerated subsonic boundary layer over the heated wall. *Int. J. Heat Mass Transf.* **2020**, *161*, 120249. [CrossRef]
18. Hajaali, A.; Stoesser, T. Flow separation dynamics in three-dimensional asymmetric diffusers. *Flow Turbul. Combust.* **2022**, *108*, 973–999. [CrossRef]
19. Fessler, J.R.; Eaton, J.K. Turbulence modification by particles in a backward-facing step flow. *J. Fluid Mech.* **1999**, *314*, 97–117. [CrossRef]
20. Hishida, K.; Nagayasu, T.; Maeda, M. Augmentation of convective heat transfer by an effective utilization of droplet inertia. *Int. J. Heat Mass Transf.* **1995**, *38*, 1773–1785. [CrossRef]
21. Pakhomov, M.A.; Terekhov, V.I. Second moment closure modelling of flow, turbulence and heat transfer in droplet-laden mist flow in a ver pipe with sudden expansion. *Int. J. Heat Mass Transf.* **2013**, *66*, 210–222. [CrossRef]
22. Ahmadpour, A.; Noori Rahim Abadi, S.M.A.; Kouhikamali, R. Numerical simulation of two-phase gas–liquid flow through gradual expansions/contractions. *Int. J. Multiph. Flow* **2016**, *79*, 31–49. [CrossRef]
23. Kopparthy, S.; Mansour, M.; Janiga, G.; Thévenin, D. Numerical investigations of turbulent single-phase and two-phase flows in a diffuser. *Int. J. Multiph. Flow* **2020**, *130*, 103333. [CrossRef]
24. Golubkina, I.V.; Osiptsov, A.N. Compressible gas-droplet flow and heat transfer behind a condensation shock in an expanding channel. *Int. J. Therm. Sci.* **2022**, *179*, 107576. [CrossRef]
25. Pakhomov, M.A.; Terekhov, V.I. Gas-droplet flow structure and heat transfer in an axisymmetric diffuser with a sudden expansion. *J. Appl. Mech. Techn. Phys.* **2020**, *61*, 787–797. [CrossRef]
26. Drew, D.A. Mathematical modeling of two-phase flow. *Ann. Rev. Fluid Mech.* **1983**, *15*, 261–291. [CrossRef]
27. Reeks, M.W. On a kinetic equation for the transport of particles in turbulent flows. *Phys. Fluids A* **1991**, *3*, 446–456. [CrossRef]
28. Derevich, I.V.; Zaichik, L.I. Particle deposition from a turbulent flow. *Fluid Dyn.* **1988**, *23*, 722–729. [CrossRef]
29. Wu, H.; Yang, C.; Zhang, Z.; Zhang, Q. Simulation of two-phase flow and syngas generation in biomass gasifier based on two-fluid model. *Energies* **2022**, *15*, 4800. [CrossRef]
30. Zeng, Y.; Xu, W. Investigation on bubble diameter distribution in upward flow by the two-fluid and multi-fluid models. *Energies* **2021**, *14*, 5776. [CrossRef]
31. Fadai-Ghotbi, A.; Manceau, R.; Boree, J. Revisiting URANS computations of the backward-facing step flow using second moment closures. Influence of the numerics. *Flow Turbul. Combust.* **2008**, *81*, 395–410. [CrossRef]
32. Elgobashi, S. On predicting particle-laden turbulent flows. *Appl. Scient. Res.* **1994**, *52*, 309–329. [CrossRef]
33. Lin, S.P.; Reitz, R.D. Drop and spray formation from a liquid jet. *Ann. Rev. Fluid Mech.* **1998**, *30*, 85–105. [CrossRef]
34. Elgobashi, S. An updated classification map of particle-laden turbulent flows. In *IUTAM Symposium on Computational Approaches to Multiphase Flow, Fluid Mechanics and Its Applications*; Balachandar, S., Prosperetti, A., Eds., Springer: Dordrecht, The Netherlands, 2006; Volume 81, pp. 3–10.
35. Mukin, R.V.; Zaichik, L.I. Nonlinear algebraic Reynolds stress model for two-phase turbulent flows laden with small heavy particles. *Int. J. Heat Fluid Flow* **2012**, *33*, 81–91. [CrossRef]